2013

Effect of the strengthened western Pacific subtropical high on summer visibility decrease over eastern China since 1973

Wenjun Qu
Ocean University of China, quwj@ouc.edu.cn

Jun Wang
University of Nebraska-Lincoln

Shanhong Gao
Ocean University of China

Tongwen Wu
China Meteorological Administration

JOURNAL OF GEOPHYSICAL RESEARCH: ATMOSPHERES, VOL. 118, 7142–7156, doi:10.1002/jgrd.50535, 2013

Effect of the strengthened western Pacific subtropical high on summer visibility decrease over eastern China since 1973

Wenjun Qu,[1,2] Jun Wang,[2] Shanhong Gao,[1] and Tongwen Wu[3]

Received 23 July 2012; revised 26 May 2013; accepted 29 May 2013; published 1 July 2013.

[1] Daily visibility (Vis) data from 354 meteorological stations are used to evaluate the seasonal Vis trends over China from 1973 to 2009, which show that Vis decline is most distinct over eastern China in summer, with a trend of −1.4 km per decade or −34% in the 37 years. This rapid decline of summertime Vis is found to be partially associated with the intensification and westward extension of the western Pacific subtropical high (WPSH) that has occurred in recent years. Such a change in the strength and breadth of WPSH has resulted in more days with stable, hot, and humid weather, which is favorable for Vis decrease. Analysis through decomposing the trend of Vis into contributions respectively from days with and without WPSH-type meteorological conditions further shows that the intensification of WPSH leads to more episodes of Vis impairment and amplifies the effect of increased aerosol and precursor emissions on the summertime Vis decline in eastern China. Consequently, the difference of Vis between summer and winter follows a declining trend, although the Vis level in winter is still lower than that in summer. The result of this study underscores the importance of considering not only the variation of anthropogenic emissions, but also the change of climate and synoptic systems in the prediction and regulation of air quality and visibility.

Citation: Qu, W., J. Wang, S. Gao, and T. Wu (2013), Effect of the strengthened western Pacific subtropical high on summer visibility decrease over eastern China since 1973, *J. Geophys. Res. Atmos.*, *118*, 7142–7156, doi:10.1002/jgrd.50535.

1. Introduction

[2] Atmospheric visibility (Vis) is inversely proportional to the volume extinction coefficient in the air [*Husar et al.*, 1981] and hence can be affected by a change of ambient relative humidity (RH) as well as by the variation in size distribution, chemical composition, and concentration of particulate matter (PM) near the surface. Long-term and statistically significant trends in Vis are usually considered to result from changes in emissions (including aerosols and their precursors, *Schichtel et al.* [2001]; *Qian et al.* [2009]). *Wang et al.* [2009] found that surface Vis during 1973–2007 has decreased globally except over parts of Europe and U.S. and attributed such regional-dependent trend of Vis to the increase of aerosol emissions in the developing countries versus continuously stricter control of emissions in the developed countries. However, it is unclear if shifts in weather patterns, possibly as a result of climate change, may have had an impact on the long-term trend of Vis on a regional to global scale. Modeling studies do show that the midlatitude air mass over North America may become more stagnant if global warming were to continue in the next 50–100 years, leading to more frequent days of poor air quality [*Jacob and Winner*, 2009]. Study on the correlations between fine PM and meteorological variables in the United States also found that PM concentrations are higher on stagnant days [*Tai et al.*, 2010]. We demonstrate here that changes in weather patterns may have combined with increases in emissions to cause Vis degradation in summer over eastern China during the last three decades.

[3] Economic growth along with urbanization and industrialization has brought an increase in energy consumption and air pollution in China, leading to more frequent days with poor Vis [*Che et al.*, 2007], particularly in large cities [*Wang et al.*, 2002; *Fan et al.*, 2005; *Chang et al.*, 2009; *Zhang et al.*, 2010] and their surrounding regions [*Qiu and Yang*, 2000; *Cheung et al.*, 2005; *Deng et al.*, 2008]. Several studies have found that the degradation of Vis shows strong seasonal variations and is most distinct in the summer. *Wang et al.* [2002] identified the summertime Vis impairment versus wintertime Vis improvement in Beijing during 1980–2000. The Vis decline was also the largest in summer for 11 cities of Hebei province during 1960–2002 [*Fan et al.*, 2005]. While past studies have revealed interesting seasonal variations of Vis degradation in China, two important questions still remain. The first is whether or not the strong degradation of Vis in summer is indeed representative of most stations in China and is it statistically significant. The second question is

Additional supporting information may be found in online version of this article.

[1]Physical Oceanography Laboratory, Key Laboratory of Ocean-Atmosphere Interaction and Climate in Universities of Shandong, Ocean University of China, Qingdao, China.
[2]Department of Earth and Atmospheric Sciences, University of Nebraska-Lincoln, Lincoln, Nebraska, USA.
[3]National Climate Center, China Meteorological Administration, Beijing, China.

Corresponding author: W. Qu, Physical Oceanography Laboratory, Key Laboratory of Ocean-Atmosphere Interaction and Climate in Universities of Shandong, Ocean University of China, Qingdao 266100, China. (quwj@ouc.edu.cn)

2169-897X/13/10.1002/jgrd.50535

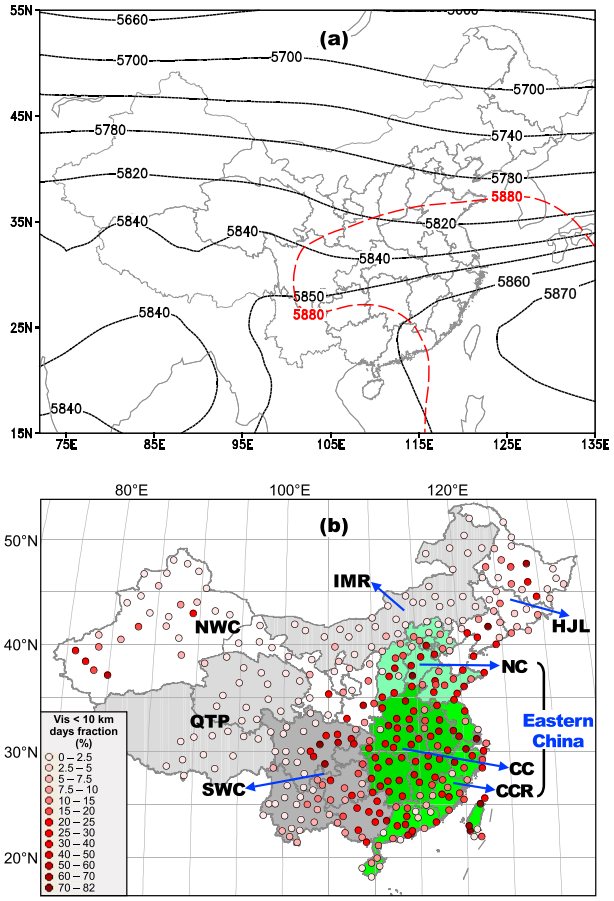

Figure 1. (a) The black contour lines show summer (June-July-August) mean geopotential height (gpm) at 500 hPa during 1973 – 2009, indicating the climatic average of WPSH. The 5880 gpm geopotential height contour at 500 hPa at local time 8 A.M., 24 July 2003 (shown in red) is used as an example to illustrate the possible variability of location and extension of WPSH. All data in Figure 1a is from NCEP global reanalysis (http://www.esrl.noaa.gov/psd/data/gridded/data.ncep.reanalysis.pressure.html). (b) Locations of the 354 Chinese meteorological stations and partition of the regions (area shaded with light green—Northern China (NC), green—Coastal China Region (CCR), and dark green—Central China (CC) is eastern China). Color of the station symbol indicates the fraction (in %) of the days with Vis < 10 km in the total days during 1973 – 2009.

whether changes in weather patterns contribute to the more distinct Vis decreases that have been observed in summer in eastern China. To date, we lack sufficient data and information for assuming emission trends on a seasonal scale; however, it is reported that emissions are generally smaller in summer compared to other seasons [*Streets et al*., 2003, Figure 7; *Zhang et al*., 2009, Table 9]. In this context, it is important to find the possible effect of changes in weather patterns, which may have acted together with the effect of changes in emissions to result in the more distinct Vis degradation in summer.

[4] The goal of this paper is to systematically study the seasonal trend of Vis in China during 1973 – 2009 and to show that the large degradation of summertime Vis over eastern China may also be related to the intensification and westward extension of the western Pacific subtropical high (WPSH) since the late 1970s [*Hu* 1997; *Chang et al*., 2000; *Gong and Ho*, 2002; *He and Gong*, 2002; *Zhou et al*., 2009]. Similar to the Atlantic Bermuda high pressure that is a key agent affecting the summer weather and the occurrence of haze over the southeastern United States [*Corfidi*, 1996], the variations of WPSH can significantly influence the distribution of summer precipitation and weather patterns in eastern China [*Tao and Xu*, 1962]. Climatologically, WPSH usually persists over the southeast part of China during summer (Figure 1a). However, it also has some significant day-to-day and interannual variations, and its 5880 gpm (geopotential height in meters) contour, an indicator often used to map WPSH spatial coverage, can intrude deep to the west and north part of China (red line in Figure 1a). The intensification and westward expansion of WPSH usually brings a long duration of hot and humid weather over eastern China [*Gao et al*., 2005]. The atmospheric subsidence associated with WPSH can often result in a stagnant air mass hovering over eastern China for weeks, creating favorable conditions for the formation and persistence of mist/haze as well as hot and humid weather near the surface. This particular summer weather phenomenon, often called "sauna weather" in China, has been shown to exhibit an increasing occurrence [*Gao et al*., 2005], but its link to the surface Vis has not been established climatologically.

[5] In this study, we evaluate the seasonal Vis variations over China from 1973 to 2009 and identify the influence of the intensification of WPSH, which can add to the effect of increased emission and PM concentration and result in the distinct summertime Vis decrease over eastern China. We describe the data in section 2 and present the occurrence of poor Vis days and seasonal Vis trends in section 3. The role of meteorology in Vis decline is discussed in section 4, which starts with the analysis of changes of RH and surface wind speed associated with WPSH (section 4.1), followed by the study of the relative role of PM concentration and RH in regulating Vis change (section 4.2); the trends of Vis and WPSH are compared in section 4.3, and all the results are then used to guide our separation of the effects of emission change and RH change in interpretation of the Vis decline in summer (sections 4.4 and 4.5). The paper is concluded in section 5.

2. Data and Partition of the Study Area

2.1. Vis and Meteorological Data

[6] The Vis, surface wind speed, temperature, and RH data are extracted from the Global Summary of Day (GSOD) database distributed by the National Climatic Data Center (ftp://ftp.ncdc.noaa.gov/pub/data/gsod). The GSOD data have already undergone extensive automated quality control and have been widely used in Vis studies [*Chang et al*., 2009; *Wang et al*., 2009].

[7] Vis was observed at more than 600 meteorological stations in China. Professional observers measured the visual range using reference objects at known distances. Daily Vis was averaged by using a minimum of four observations per day with an uncertainty of 0.1 km [*China Meteorological Administration*, 2003]. This study uses data from 354 stations (Figure 1b) during 1973 to 2009, where and when data sets are most complete.

2.2. PM_{10} Concentration Data

[8] This study also uses PM_{10} (particulate matter ≤ 10 μm) concentration data at 86 Chinese cities from 2000 to 2009. These data are derived from the Air Pollution Index records (reported daily by the State Environmental Protection Agency of China, available at http://www.sepa.gov.cn/quality/air.php3) using the method described by *Qu et al.* [2010]. We investigated the relationship of Vis and PM_{10} concentration for 52 stations, where the PM_{10} concentration was measured at cities located within 0.5° (both latitude and longitude) of the Vis observation stations.

2.3. WPSH Intensity and Western Limit Index Anomaly

[9] The National Climate Center of China (NCCC) has distributed WPSH indices (including the area index, the intensity index, the west boundary, the position of ridge, and the north boundary) since the 1970s [*He and Gong*, 2002]. However, the continuity of these indices is not reliable due to inconsistent error sources associated with changes of the method used to calculate these indices [*Gong et al.*, 1998; *He and Gong*, 2002].

[10] With the correction of these errors, *Mu et al.* [2001] reconstructed WPSH indices based upon the 500 hPa geopotential height data set and WPSH indices distributed by the NCCC, and calculated yearly anomaly of the intensity index (AII) and anomaly of the western limit index (AWI) of WPSH in summer from 1880 to 1999. Since these anomalies are shown to be robust for the characterization of WPSH intensity and area coverage [*Mu et al.*, 2001], they are used in this study. We also computed WPSH indices for years after 1999 using the United States National Centers for Environmental Prediction reanalysis data [*Kalnay et al.*, 1996] and include these indices in the study to facilitate analysis of the relationship of WPSH, meteorology, and Vis.

[11] The higher intensity index and the lower (more negative) value of the western limit index usually indicate a stronger WPSH. It should be noted that the western limit index of WPSH is defined here as the longitude of the westernmost tip of the 5880 m contour line on the map of 500 hPa geopotential height. Hence the anomaly of the western limit index of WPSH each year reflects the deviation of the WPSH western boundary in that year from its climatological (1961 – 1990) mean [*Mu et al.*, 2001]. The smaller (or more negative) this anomaly value, the farther west WPSH extends, meaning that WPSH intrudes deeper west into mainland China and thus covers more of eastern China. As expected, a strong negative correlation exists between AWI and AII ($R^2 = 0.70$, $n = 27$, $P < 0.0001$ significance), indicating that intensification of WPSH is often accompanied by its westward expansion, both of which can result in increased stable weather over larger areas in eastern China. Another index, the WPSH ridge index, is defined as the latitudinal position of the WPSH ridge; the larger (or more positive) the anomaly of this index, the farther north WPSH is located; i.e., WPSH is displaced northward into mainland China and therefore covers more of eastern China.

[12] As the western limit index varies oppositely with the intensity and the coverage of WPSH, directly using the value or the AWI may lead to misunderstanding. For the convenience of discussion, we use the negative AWI (NAWI) and the AII hereafter in the paper. NAWI and AII vary consistently with the WPSH. That is, the larger their value, the more intensive WPSH is and the more coverage of WPSH over eastern China.

2.4. Partition of the Study Area

[13] The study area and the meteorological stations are partitioned into eight regions (Figure 1b). Among them, Northern China (NC, 36 stations) includes Beijing and Tianjin Municipalities, Hebei, Shanxi, and Shandong Provinces. Central China (CC, 45 stations) includes Henan, Hubei, Hunan, Anhui, and Jiangxi Provinces. Coastal China Region (CCR, 55 stations) includes Jiangsu, Zhejiang, Fujian, Guangdong, and Hainan Provinces, Shanghai Municipality, Hong Kong and Macao Special Administrative Regions, and Taiwan. Note the areas including NC, CC, and CCR (136 stations) are also mentioned as eastern China in this paper. The other five regions are SouthWestern China (SWC, 68 stations) including Sichuan, Yunnan, and Guizhou Provinces, Chongqing Municipality, and Guangxi Zhuang Autonomous Region; Heilongjiang, Jilin and Liaoning Provinces (HJL, 39 stations); NorthWestern China (NWC, 48 stations) including Xinjiang Uygur Autonomous Region, Gansu, Ningxia, and Shaanxi Provinces; Inner Mongolia Autonomous Region (IMR, 34 stations); and Qinghai-Tibet Plateau (QTP, 29 stations) including Qinghai Province and Tibet Autonomous Region.

3. Occurrence of Days With Vis < 10 km and Seasonal Vis Trends

[14] According to the meteorological standard of China [*China Meteorological Administration*, 2010], 10 km is the minimum Vis value for Vis to be graded as "fine" on a given day. Hence, any day with Vis < 10 km is considered as a poor-Vis day in this study. The stations with more than 5% poor-Vis days in 37 years (1973–2009) are mostly concentrated in eastern China (including NC, CC, and CCR) and the eastern part of SWC, and are more scattered in HJL and the western and eastern parts of NWC (Figure 1b). This geographical distribution of poor-Vis regions is consistent with the areas that have large anthropogenic emissions and high population density [*Streets et al.*, 2003; *Zhang et al.*, 2009].

[15] The 25th percentile Vis in each season for every year is used here to estimate the 1973 – 2009 seasonal trend of Vis because: (1) low Vis values are the major focus as they best reflect Vis degradation and (2) the visual range generally can be estimated more accurately under low Vis conditions than under high Vis conditions [*Zhu and Mei*, 2010]. *Li* [2010] also reported that the low and median values of Vis are more reliable as they are less influenced by artificial factors.

[16] Over the past 37 years, Vis degradation has occurred primarily in eastern China, HJL, and eastern SWC (Figure 2), which is also consistent with the area of intensive and rapidly increasing anthropogenic emission [*Streets et al.*, 2003; *Zhang et al.*, 2009]. For the whole country, 185 and 173 stations experienced Vis decreases (−2.0 and −1.8 km per decade, respectively) in summer and autumn (Figures 2b and 2c), while 126 and 102 stations experienced Vis increases (+1.5 and +1.3 km per decade, respectively) in spring and winter (Figures 2a and 2d). All these trends are significant at the 95% confidence level. The significant declining trend in summertime Vis at most stations in eastern China is especially noteworthy.

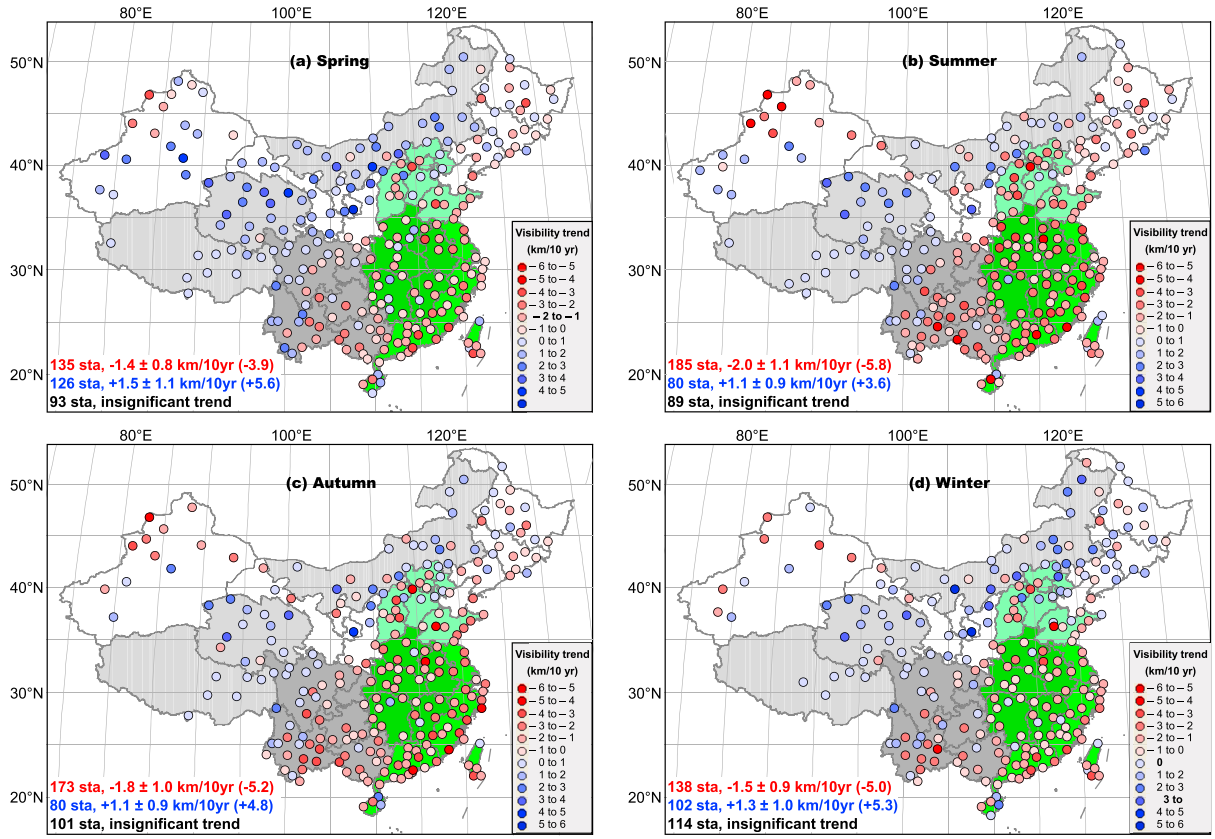

Figure 2. Geographical distribution of trends of 25th percentile Vis (km/10yr, km per decade) from 1973 to 2009 for (a) spring (March, April, May), (b) summer (June, July, August), (c) autumn (September, October, November), and (d) winter (December, January, February). The bottom left of each panel shows statistics of the trends, including the number of stations, averaged trend ± standard deviation km/10yr (the extrema of the negative or positive trends). All shown and counted trends are significant at 95% confidence level.

[17] To evaluate if the Vis decrease is indeed greater in summer, we calculate the relative difference of Vis trends between summer and winter [DVT_{S-W} = (the summertime Vis trend − the wintertime Vis trend) / the absolute value of the wintertime Vis trend, Figure 3a] for the stations which have significant ($P < 0.05$) negative summertime Vis trend and significant ($P < 0.05$) wintertime Vis trend. For the 141 stations where the DVT_{S-W} value is available, 113 stations have DVT_{S-W} more negative than −0.1. That is, at those sites, Vis has declined more in summer, and the difference of the Vis decrease between summer and winter is larger than 10% of the wintertime Vis trend. The DVT_{S-W} is more negative than −0.1 for most of the stations in eastern China, revealing a more distinct Vis decrease in summer in that region (Figure 3a).

[18] Figure 3b illustrates the 141 stations which have the most negative Vis trend in summer (among the four seasons), showing that most of the stations in eastern China have seen the largest Vis decreases in summer. The combined results in Figures 3a and 3b answer the first question posed in section 1; in short, strong summertime Vis degradation is indeed representative of most stations in eastern China.

[19] Figure 3c clearly demonstrates that the Vis decline in summer (−1.4 km per decade, −34% in 37 years) is more rapid than that in winter (−0.73 km per decade, −25% in 37 years) over eastern China. Consequently, the difference of Vis between summer and winter [Vis (Summer − Winter)] decreases in Figure 3c, although Vis in winter is still lower than that in summer.

[20] Seasonal statistics over different regions also indicate greater Vis decreases over eastern China in summer and autumn (−1.4 and −1.2 km per decade, −34% and −32% for the 37 years, respectively). This amounts to about double or more than double the trends over other seasons and regions (e.g., −0.33 to −0.76 km per decade, −7.6% to −15% for the 37 years over SWC and HJL; Table 1). The analysis below will therefore focus on the decrease of Vis over eastern China and show that the distinct Vis decrease over eastern China in summer may be related to the corresponding variation of WPSH in addition to the contribution of emission increases (section 4).

[21] The larger temporal decline in summertime Vis relative to that in winter does not necessarily mean that the summertime Vis levels are lower than those in winter (Figure 3c). Our statistics show that winter Vis remains the lowest among the four seasons (possibly in part due to more intensive emissions as well as greater incidence of fog during winter) for most of the stations and areas in China. This study only focuses on the more evident Vis *decline* (both in relative and absolute value) in summer over eastern China during the 37 year period.

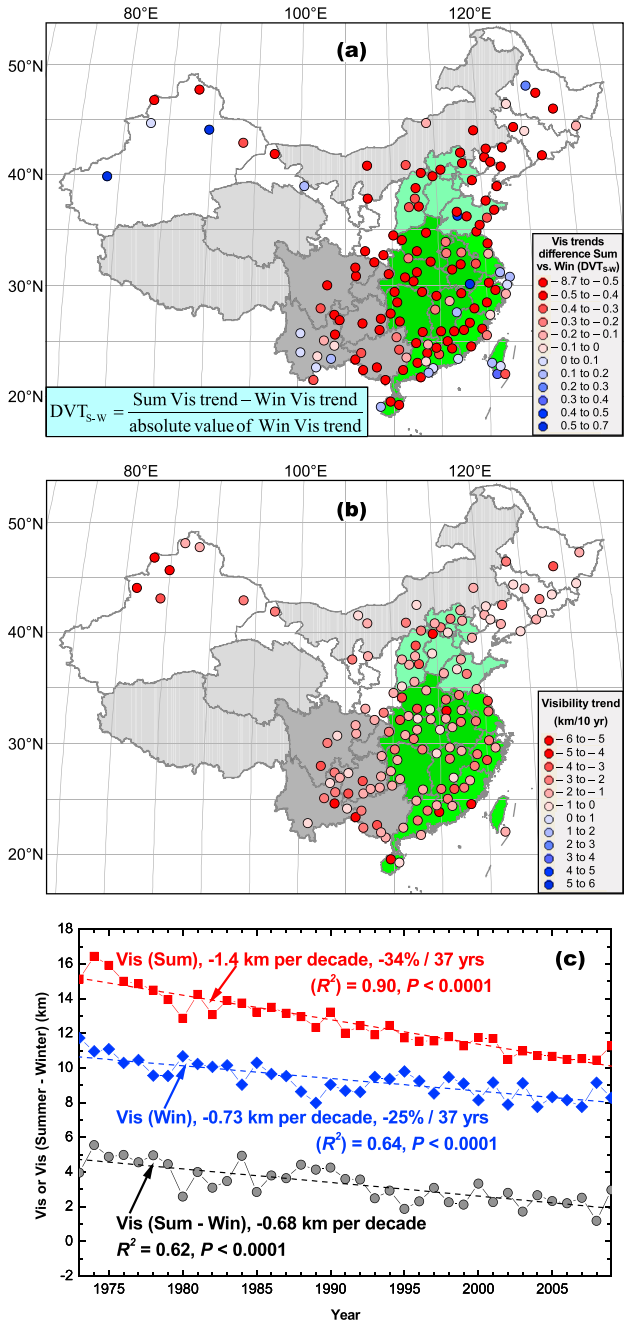

Figure 3. (a) Geographical distribution of the relative difference of the trends in the 25th percentile Vis from 1973 to 2009 between the summer and the winter, expressed as DVT_{S-W} = (the summertime Vis trend − the wintertime Vis trend) / the absolute value of the wintertime Vis trend. (b) Location of the stations at which the most negative Vis trend (among the four seasons) has occurred in summer. Color of the station symbol indicates value of the trend (significant at 95% confidence level) in the summertime 25th percentile Vis (km per decade) from 1973 to 2009. (c) 1973 – 2009 time series of summer (June-July-August) Vis, winter (December-January-February) Vis, and the difference of Vis between summer and winter Vis [Vis (Summer − Winter)] over eastern China.

4. Role of Meteorology in Vis Decline

[22] In addition to the mass concentration of dry aerosols, RH and surface wind speed are important factors that can affect the variation of Vis, and consequently their changes associated with WPSH are analyzed first.

4.1. Relationship of RH and Wind Speed With WPSH

[23] The NAWI of WPSH shows positive correlation with RH ($R^2 = 0.37$, $P < 0.001$ significance, n = 37) and negative correlation with surface maximal wind speed ($R^2 = 0.38$, $P < 0.0001$ significance, n = 37) over eastern China in summer during 1973 – 2009 (Figures 4a and 4b). On the other hand, although no significant summertime RH trend was found for the whole data set, the occurrence (number) of RH > 70% (humid) days over eastern China shows an increase trend (+2.7 day per decade, $R^2 = 0.37$, $P < 0.0001$; Figure 4c) from 1973 to 2009. Meanwhile, the summertime surface wind speed decreases (−0.10 m/s per decade, $R^2 = 0.54$, $P < 0.0001$) during the same period. These analyses imply that intensification and westward expansion of WPSH can cause more days with relatively moist, low-wind conditions in summer over eastern China, which can lead to more frequent low Vis events and is favorable for Vis decrease. It is worth noting that meteorological conditions (such as RH and wind speed) can be influenced by other factors, such as small-scale weather systems, but the focus here is the link of Vis climatology with WPSH climatology.

[24] We further evaluate RH trend for the subset of data in the range of RH > 70%, which shows that the geometric mean RH on the days with RH > 70% increases (+0.30% per decade, $R^2 = 0.38$, $P < 0.0001$; Figure 4d) from 1973 to 2009 over eastern China. As will be shown in section 4.2, for the same amount of increase (or decrease) in RH, aerosol particles grow (or shrink) much faster in high RH conditions than in low RH conditions. Therefore, this increasing trend of RH in the high value range has a larger effect on Vis decline (than that for the same amount change of RH in the low value range), which will be discussed in detail in section 4.2. (Note here the geometric mean indicates the central tendency or typical value of a set of numbers by using the product of their values (as opposed to the arithmetic mean which uses their sum)); it is defined as the nth root (where n is the count of numbers) of the product of the numbers.)

[25] For data in the range of RH < 70%, the occurrence of RH < 70% days decreases (−2.0 day per decade, $R^2 = 0.32$, $P < 0.001$) over eastern China. The RH trend for days with RH < 70% is insignificant (−0.25% per decade, $R^2 = 0.067$, $P = 0.12$).

4.2. Relative Role of PM Concentration and RH

[26] In this section, we study the relative role of PM concentration and RH in regulating the Vis change using data collected in Beijing; such analyses are also extended to other stations. Fitting between Vis and PM_{10} concentration (the black curve in Figure 5c) indicates that there is a threshold value (150 μg/m^3 in this case; shown by green dot) beyond which the increase of PM_{10}

Table 1. Statistics on the Geometric Mean of the 25th Percentile Visibility in the Four Seasons Over Eastern China, SWC, and HJL Region[a]

Region	Trend and Variation of Visibility	Spring	Summer	Autumn	Winter
Eastern China	Trend, km/10 years	−0.62	−1.4	−1.2	−0.73
	R^2	0.60	0.90	0.87	0.64
	P	<0.0001	<0.0001	<0.0001	<0.0001
	Variation, %/37 years	−19	−34	−32	−25
SWC	Trend, km/10 years		−0.76	−0.37	
	R^2		0.68	0.20	
	P		<0.0001	<0.01	
	Variation, %/37 years		−14	−8.6	
HJL	Trend, km/10 years	−0.34	−0.67	−0.33	0.23
	R^2	0.33	0.67	0.32	0.13
	P	<0.001	<0.0001	<0.001	<0.05
	Variation, %/37 years	−7.8	−15	−7.6	7.1

[a]Statistics include the Vis trend during 1973–2009, Vis correlation with time expressed as square of linear correlation coefficient R^2 and significance level P, as well as variation of Vis in the 37 years; insignificant trends are not shown. Eastern China include NC, CC and CCR as described in Section 2.4 of the main text.

concentration results in little or no change in Vis. Hence, to interpret the trend of Vis from the Vis-PM scatterplot, we should pay more attention to the range corresponding to a PM_{10} concentration $< 150\ \mu g/m^3$, hereafter called the "Vis-PM_{10} concentration Sensitive Area (VPSA)." Figure 5a (including the statistics shown on the top) indicates that in summer, a majority (about 73%) of the daily PM_{10} concentration measurements are within the VPSA; in contrast, in winter, ~45% of the PM_{10} concentration measurements are beyond VPSA. This suggests that higher PM_{10} in winter is related to low Vis, but that further increase of the already high PM concentration during this time period has only minimal impact on Vis.

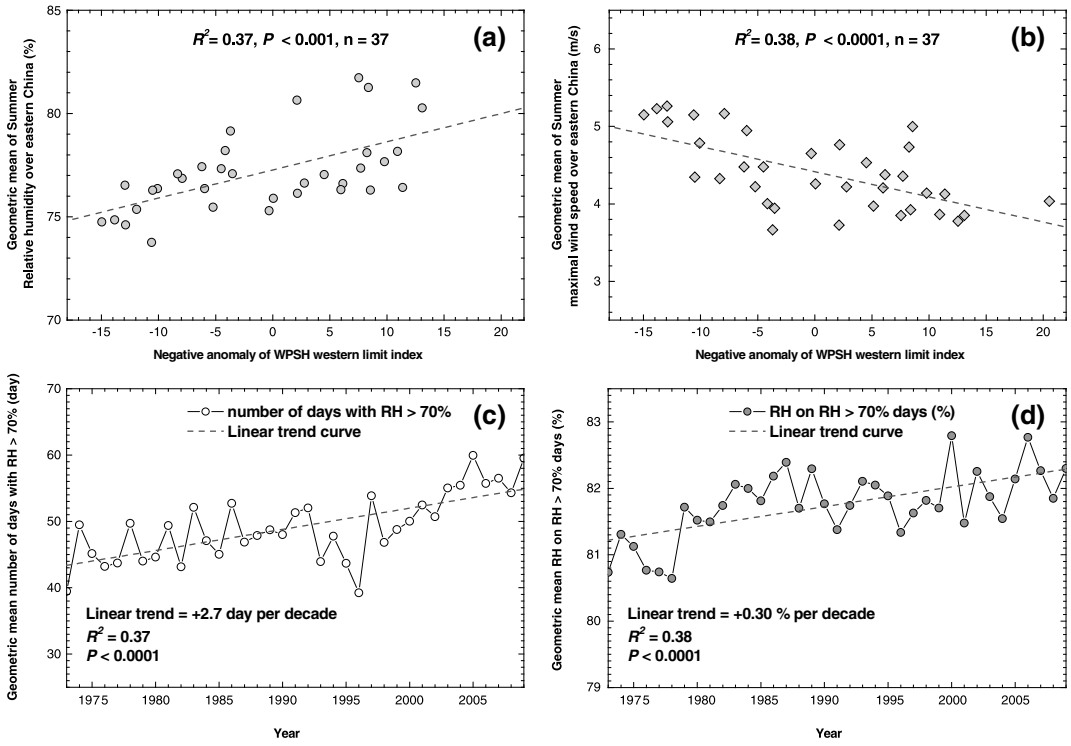

Figure 4. Scatterplots of the geometric mean of (a) relative humidity (%) and (b) surface maximal wind speed (m/s) over eastern China in summer during 1973 – 2009 (y-axis) with the negative anomaly of the western limit index (NAWI) of WPSH; the best linear fitting line (dash line) between the variations of the variables on the y-axis and x-axis is also shown. 1973 – 2009 summer (June-July-August) time series of (c) the geometric mean number of days with RH > 70% (day) and (d) the geometric mean RH on the days with RH > 70% (%) over eastern China. The geometric mean is the nth root (where n is the count of numbers) of the product of the numbers.

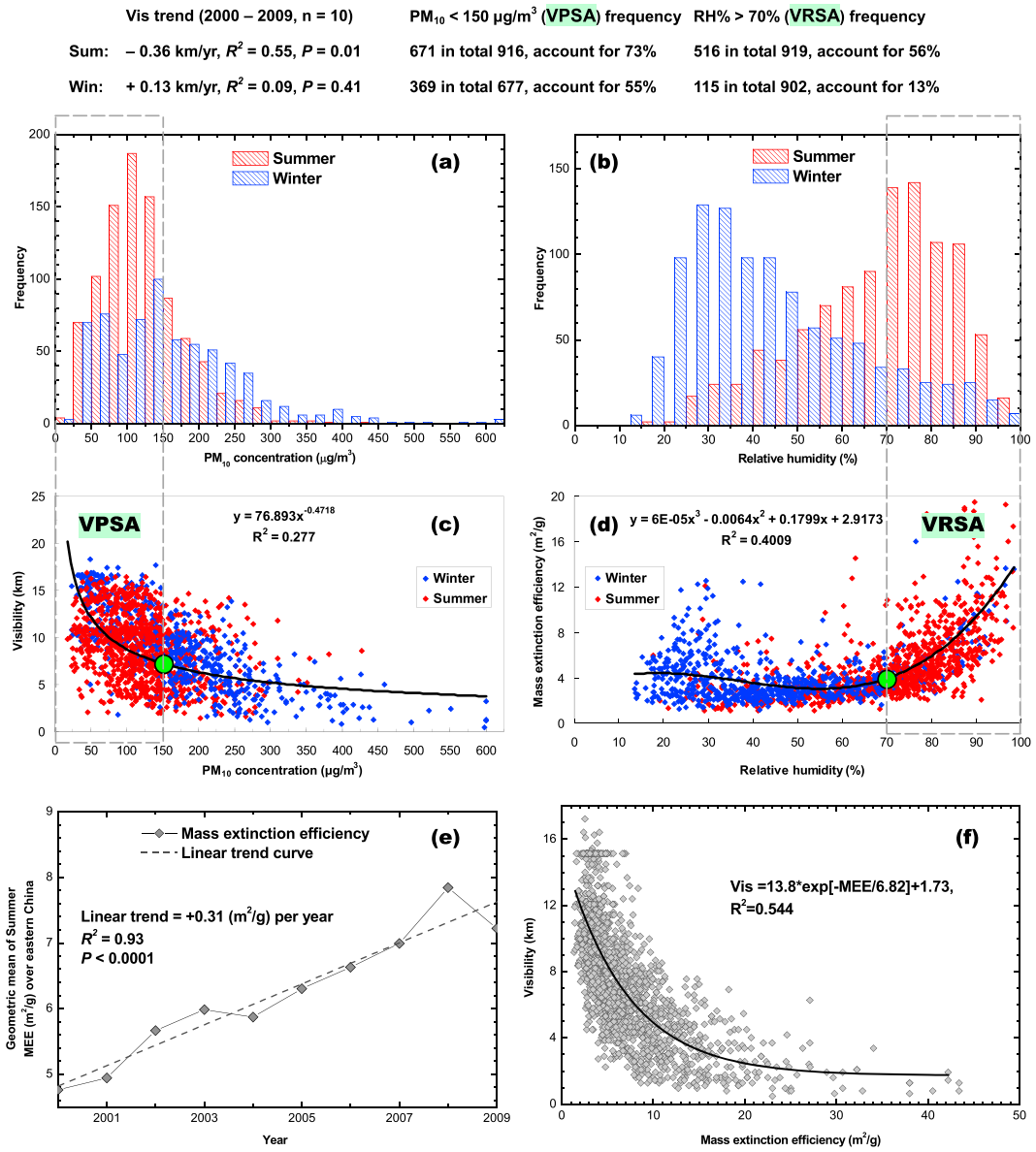

Figure 5. Contrast analysis of surface observations at Beijing in summer (shown in red) and winter (shown in blue) during 2000 – 2009. (a) Frequency distribution of the surface PM_{10} mass concentration for summer and winter. (b) Same as Figure 5a but for surface relative humidity (RH). (c) The relationship and correlation (shown as R^2) between daily surface Vis and PM_{10} mass concentration; the black curve is the line fitted to the data, and the green dot indicates the threshold for PM_{10} concentration value (150 μg/m^3 in this case) below which a specific increase of the PM_{10} concentration can cause much larger Vis decline [i.e., the "Vis-PM_{10} concentration Sensitive Area (VPSA)"] than beyond this threshold. (d) Same as Figure 5c but for daily mass extinction efficiency (MEE) and RH, the green dot indicates the threshold of RH value (70% in this case) beyond which a specific increase of the RH can cause much larger MEE increase [usually corresponding to Vis decline, i.e., the "Vis-RH Sensitive Area (VRSA)"] than below this threshold. Also shown on the top of the figure are the statistics for Vis trend as well as number (proportion) of daily PM_{10} concentration and RH measurements within the VPSA and the VRSA, respectively, in summer and winter. (e) 2000 – 2009 summer (June-July-August) time series of the geometric mean of MEE over eastern China. (f) The relationship and correlation (shown as R^2) between daily surface Vis and MEE at Beijing in summer and winter during 2000 – 2009; the black curve is the line fitted to the data. For the definition of geometric mean, refer to section 4.1 and Figure 4.

[27] Besides dry PM mass, surface RH, through its effect on aerosol hygroscopic growth [*Wang et al.*, 2008], is another compounding factor influencing Vis variation. To investigate how Vis is affected by both PM_{10} and RH, the mass extinction efficiency (MEE) of dry aerosol, defined as the ratio of the extinction coefficient to the PM_{10} mass concentration [*Si et al.*, 2005], is also computed. In this calculation, the light extinction is derived from Vis based upon the Koschmieder's formula:

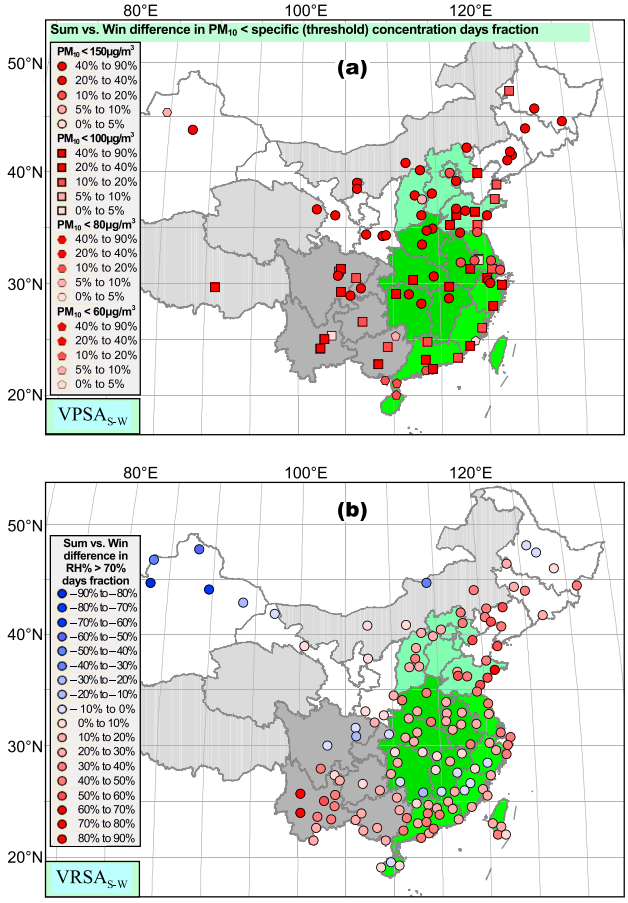

Figure 6. (a) Geographical distribution of summer and winter difference (in fraction or percent of days) that have PM_{10} < specific concentration (similar to the threshold PM_{10} value shown in Figure 5c) at 86 Chinese cities during 2000 – 2009, which reflects the difference in fraction of VPSA between summer and winter ($VPSA_{S-W}$). (b) Same as Figure 6a but for days with RH > 70% (similar to the threshold RH value shown in Figure 5d) at Vis observation stations during 1973 – 2009, which reflects the difference in fraction of VRSA between summer and winter ($VRSA_{S-W}$).

$$\sigma_{ext} = 3.912/V, \quad (1)$$

where σ_{ext} is the volume extinction coefficient and V denotes Vis (in km).

[28] In comparison to the finding of VPSA in Figure 5c, the scatterplot between the MEE and the RH in Figure 5d indicates an RH threshold (70% in this case; shown by green dot) beyond which a small increase of RH can cause a much larger MEE increase (usually corresponding to Vis decline; see Figure 5f). Hereafter, the range where the corresponding RH is 70% or larger in the MEE-RH scatterplot is called the "Vis-RH Sensitive Area (VRSA)." Within this VRSA, the size of the hygroscopic aerosols grows sharply after RH is larger than the deliquescent RHs of 70–80% [*Wang et al.*, 2008], subsequently resulting in an increase in the aerosol extinction coefficient and a decrease in Vis. One can see clearly in Figure 5f that Vis declines as MEE increases. During 2000 to 2009, when the MEE data are available (due to PM_{10} data available then), the geometric mean of summertime MEE over eastern China shows a significant increase trend (+0.31 m^2/g per year, $R^2 = 0.93$, $P < 0.0001$; Figure 5e). This increase trend in MEE corresponds to the declining Vis trend (−0.15 km per year, $R^2 = 0.63$, $P < 0.05$) occurring at the same time. The summertime MEE trend at Beijing (+0.36 m^2/g per year, $R^2 = 0.57$, $P < 0.05$) is similar.

[29] In contrast to the low wintertime proportion of 13%, in summer, about 56% of days have daily RH values within VRSA (Figure 5b and the statistics on the top in Figure 5). As MEE (and subsequently Vis) is disproportionately related to RH (Figure 5d), it is likely that the larger Vis decline in summer is partially due to the greater number of high RH days (i.e., daily RH value within VRSA) in summer than in winter, because within VRSA, MEE (and subsequently Vis) shows a much larger response to a change in RH (than that for a same amount of RH change in the low value range; Figures 5d and 5f).

[30] Figure 5 suggests that interpretation of Vis trends should consider both changes in atmospheric PM mass concentration (or emissions) and changes in RH. Both aspects are explored for each Vis station by first examining the difference in the percentage of days in which PM mass is in the VPSA between summer and winter (hereafter $VPSA_{S-W}$). As shown in Figure 6a, $VPSA_{S-W}$ is larger than 10% for most of the cities, indicating that a larger proportion of PM_{10} concentrations below the threshold PM_{10} value (i.e., within the VPSA) occur in summer than in winter. Similarly, Figure 6b shows that at most stations, the difference in fraction of VRSA between summer and winter, or $VRSA_{S-W}$, is also generally larger than 10%; this implies that more days have an RH larger than 70% (i.e., RH within the VRSA) in summer than in winter. Such paired differences (of RH and PM) between summer and winter all favor a hypothesis that the increased occurrence of high RH (humid) and low wind speed days (i.e., stable weather days, generally accompanied by accumulation of atmospheric PM within the boundary layer) as a result of WPSH intensification (as presented in Figure 4 and discussed in section 4.1) may contribute to the larger Vis decline trend in summer than that in winter. While this conjecture will be further verified in the following two sections, it is noted that a higher proportion of days with relatively lower aerosol concentration and higher RH values during summer is consistent with many past investigations about the seasonal variation of the aerosol concentration [*Zhang et al.*, 2008; *Qu et al.*, 2010; *Zhang et al.*, 2012] and the typical seasonal variation of RH due to the monsoon climate over eastern China.

[31] Although we evaluated the variation of Vis with RH through their links with MEE (Figures 5d and 5f), one may also consider the direct relationship between Vis and RH. While the daily Vis shows significant negative correlation with the daily RH (for example, $R^2 = 0.44$, $P < 0.0001$, $n = 1821$ at Beijing in summer and winter during 2000 – 2009), the seasonal statistics of Vis and RH show no significant correlation. This is probably due to the loss of information during the averaging process. Note here the daily Vis and RH data already are of comparably coarse resolution. Moreover, the daily RH actually varies in a very limited range, and further statistical analysis of this daily data can lead to additional loss of RH variation information.

[32] Finally, as indicated in section 4.1, although there is no significant summertime RH trend for the whole data set, the RH trend for the subset of data in the range of

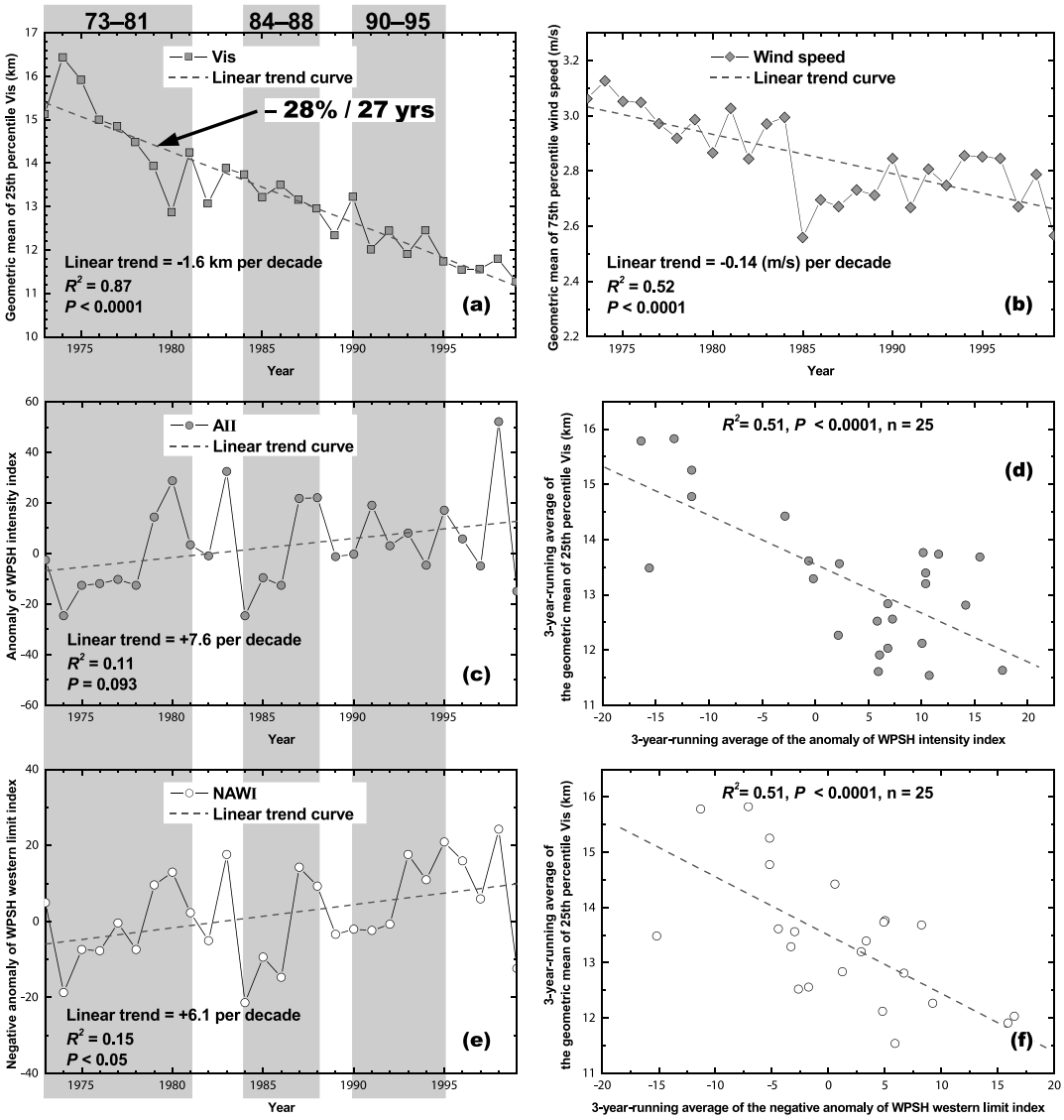

Figure 7. 1973 – 1999 summer (June-July-August) time series of (a) the geometric mean of 25th percentile Vis, (b) the geometric mean of 75th percentile wind speed, (c) the anomaly of the intensity index (AII) of WPSH, and (e) the negative anomaly of the western limit index (NAWI) of WPSH over eastern China. Scatterplots of the 3 year running average of the geometric mean of the 25th percentile summertime Vis (y-axis) with (d) the 3 year summer running average of AII, and (f) the 3 year summer running average of NAWI during 1973 – 1999; the best linear fitting line (dash line) between the variations of the variables on the y-axis and x-axis is also shown. For the definition of geometric mean, refer to section 4.1 and Figure 4.

RH > 70% (i.e., the RH trend on the days with RH > 70%) increases significantly (Figure 4d) from 1973 to 2009 over eastern China. From Figure 5d and the discussion in section 4.2, we know that the relationship between Vis and RH is nonlinear and that an equal amount increase of RH in the high value (RH > 70%) range (i.e., VRSA) can result in a much larger Vis decline than in the low value range. Therefore, the increase trend of RH on the days with RH > 70% (i.e., an increase of RH *within VRSA*) can lead to more obvious Vis decrease than the effect of an equal change of RH in the low value range.

4.3. Trends of Vis and WPSH Index

[33] WPSH is a major synoptic system that results in thermodynamically stable weather. These stable weathers can lead to accumulation of atmospheric particles and high RH, both of which favor Vis decrease in summer. In this section, the time series of Vis over eastern China is compared with the variation of WPSH (Figure 7) to find possible link between them.

[34] Summertime Vis over eastern China shows a declining trend from 1973 to 1999 (decreases 28% for the 27 years, Figure 7a), while the AII of WPSH increases (Figure 7c) and the NAWI of WPSH increases (Figure 7e) during the same course. More specifically, during three periods, or during 20 of the total 27 years in our analysis (1973 – 1981, 1984 – 1988, and 1990 – 1995; gray shading in Figures 7a, 7c, and 7e), summertime Vis over eastern China (Figure 7a) shows opposite variations with AII (Figure 7c) and generally opposite variations with NAWI (Figure 7e). Moreover, the higher Vis in 1974 (Figure 7a) is corresponding to the weaker

WPSH (Figure 7c) and eastward retreat of WPSH (Figure 7e), while the lower Vis in 1980 (Figure 7a) is corresponding to the stronger WPSH (Figure 7c) and westward extension of WPSH (Figure 7e). These results indicate that the summertime Vis decrease over eastern China is consistent with the intensification and westward expansion of WPSH.

[35] Quantitatively, the summertime Vis shows significant negative correlation with AII ($R^2 = 0.18$, $P < 0.05$ significance, n = 27) and NAWI ($R^2 = 0.20$, $P < 0.05$ significance, n = 27) during 1973 – 1999. However, while statistically significant, the relatively small R^2 (~0.20) between Vis and WPSH may result from the following factors: (1) the domain used to determine the WPSH index is similar but not equal to the eastern China area within which we evaluate the Vis trend, (in sections 4.4 and 4.5, we will conduct more detailed analysis based upon daily meteorology at each station); and (2) the Vis trend is influenced by both the change of PM concentration (emission) and the change of RH caused by WPSH (as discussed in section 4.2 and will be discussed in sections 4.4 and 4.5); therefore, the correlation between Vis and WPSH index only partially explains the variance in Vis. In addition, the noise of the interannual variation of WPSH can obscure its long-term effect on Vis. Indeed, the 3 year running average (to remove influence/noise from interannual fluctuation) of summertime Vis shows stronger correlations ($R^2 = 0.51$, $P < 0.0001$ significance, n = 25) with the 3 year running average of AII (Figure 7d) and NAWI (Figure 7f) during 1973 – 1999. For a more complete time series (from 1973 to 2009, with our computed WPSH indices for years after 1999 included in the analysis), the summertime Vis shows better correlation with the WPSH indices; the R^2 values for correlations between Vis over eastern China and NAWI and the anomaly of the WPSH ridge index are 0.47 and 0.52, respectively ($P < 0.0001$ significance, n = 37). These statistics further support the notion that the intensification and westward expansion of WPSH favor summertime Vis decrease over eastern China.

[36] We find that the summertime wind speed also declined from 1973 to 1999 (Figure 7b). This is consistent with *Xu et al*. [2006], who reported on the steady decline of mean surface wind speed from 1969 to 2000. Meanwhile, summertime Vis shows significant positive correlation with surface wind speed ($R^2 = 0.38$, $P < 0.0001$ significance, n = 37) over eastern China during 1973 to 1999. Hence, the analysis of trends and variation of Vis, wind, and WPSH in Figure 7 reveals that the stable, humid, and low-wind weather under WPSH is likely to contribute to low Vis. However, the influence of emission increases on Vis variation should be eliminated before the role of RH in the rapid decline of summertime Vis can be confirmed. Therefore, in the next two sections, we focus on separating the effect of RH (as a result of WPSH intensification) from the effect of emission changes on summertime Vis decline.

4.4. Trend of Days With WPSH-Type Meteorology in Summer

[37] To date, a yearly continuous series of season-by-season aerosol emissions is not available on a global scale, and this kind of data over China on the *regional* scale is neither available nor possible for our study period because some of the data (such as fossil fuel usage, and land use or agriculture practice in each province) needed for emission estimates were not collected between the 1970s and 1990s. Therefore, although it is clear that total energy consumption in China has increased by ~399% from 1978 to 2008 (571 → 2850 million tons standard coal equivalent, increased 13.3% per year, National Bureau of Statistics China, http://www.stats.gov.cn/tjsj/ndsj/2009/indexch.htm), quantitatively estimating the effect of increasing emissions on Vis decline is challenging. However, the proportion of anthropogenic emissions of major pollutants in summer is generally less than that in winter [see *Streets et al*., 2003, Figure 7 and *Zhang et al*., 2009, Table 9]. Disparity between the seasonality of the (summertime larger) decline trend in Vis and the (summertime less) emission rate suggests that meteorology should be considered in addition to emission rates in order to explain the greater Vis decreases that have occurred in summer versus winter.

[38] To further test our hypothesis that the increase of days with higher RH as a result of WPSH intensification is an integral part of the summertime Vis decrease, we first define the typical WPSH-controlled day as: (1) daily average temperature > 28°C, (2) daily average RH > 75%, and (3) surface wind speed < the summertime average in the concurrent year. These criteria are chosen because the weather under WPSH control is characterized by heat, humidity, and weak convection (low wind speed). The temperature and RH criteria used here are consistent with those used by *Xu et al*. [2008]. Note here the RH > 75% criterion is comparable to the RH threshold for the "VRSA" discussed in section 4.2, and it is also in the range of the deliquescent RHs of 70–80% beyond which the size of hygroscopic aerosols grows sharply [*Wang et al*., 2008] and subsequently results in an increase of the aerosol extinction coefficient and a decrease in Vis. However, at some stations over the mountains, the temperature criterion of >25°C is used to account for the low temperatures commonly observed at higher elevations; likewise, for the stations in the coastal region (CCR), an RH criterion of >85% is used to accommodate the higher RH common to coastal regions in summer, and for stations in the dry interior, an RH criterion of >65% is used. It is also reported that "the average RH is about 60% to 86% accompanied with high temperature, lower wind speed as well as less precipitation" for major cities over eastern China under the control of WPSH in summer [*Zhang et al*., 2004]. This is consistent with our defined criteria for a WPSH-controlled day. As expected, Figure 8a shows that the Vis difference (ΔVis) between summer (June, July, and August) days controlled and not controlled by WPSH is negative for all the stations, and ΔVis is often less than −1 km (ΔVis < −1 km) for most stations in eastern China. Such large Vis contrast suggests that the stable weather associated with WPSH is a major cause of Vis decrease over eastern China in summer, which is more important during summertime than the fog/rain associated with the passing midlatitude disturbances. We also calculate the number (frequency) of WPSH-type weather Vis impairment (Vis less than a specific value) days for individual stations. For most stations over eastern China, the number of Vis impairment days accompanied by typical WPSH-controlled weather near the surface increases by at least 35 from the first decade (1973 – 1982) to the last decade (2000 – 2009) of our study period (Figure 8b). Moreover, the annual number (frequency) of WPSH-type weather Vis impairment days over eastern China exhibits an increasing trend of +2.3 days per

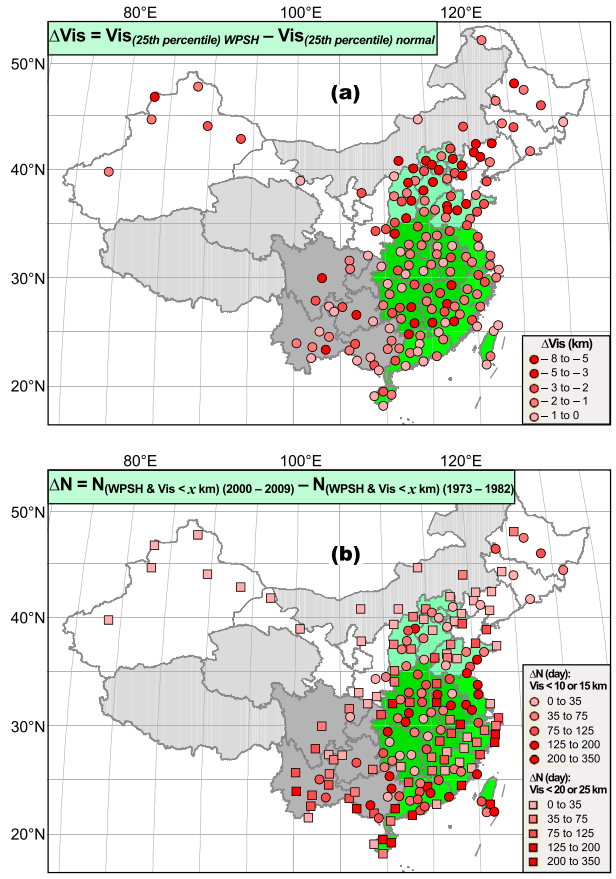

Figure 8. (a) Geographical distribution of the difference of the 25th percentile Vis (denoted as ΔVis) between days with WPSH-type weather (stable / weak wind, hot and humid) days and normal days (without WPSH-type weather) in summer (June, July, August) during 1973 – 2009. (b) Geographical distribution of the difference between the last decade (2000 – 2009) and the first decade (1973 – 1982) in total number of days (denoted as ΔN) with both WPSH-type weather and Vis less than a specific value (manually selected for each individual station) in summer.

decade (Figure 9a). These results are consistent with the observed intensification and westward extension of WPSH since the late 1970s [*Hu* 1997; *Chang et al*., 2000; *Gong and Ho*, 2002; *He and Gong*, 2002; *Zhou et al*., 2009], and they further support our analysis in section 4.3 about the consistency and reasonable relationship between decreased summertime Vis and the strengthening of WPSH that has occurred since the late 1970s. Consequently, we conclude that the increasing number of "WPSH-type weather Vis impairment days" has contributed to the greater Vis decline that has been observed over eastern China in summer since 1973.

4.5. Quantitative Link Between Vis Decline and WPSH

[39] To quantitatively evaluate the contribution of WPSH to Vis decline, we can describe the average Vis in a given summer as being the sum of Vis on "normal" days (the days without WPSH weather) and Vis on WPSH-controlled days, weighted by the number of their respective total days in the summer:

$$Vis = Vis_{normal} \times (N - N_{WPSH})/N + Vis_{WPSH} \times N_{WPSH}/N \quad (2)$$

where Vis is the visibility in a specific year, Vis_{normal} is Vis on the normal days, Vis_{WPSH} is Vis on the days with WPSH-type meteorology, N_{WPSH} is the count of the days with WPSH-type meteorology, and N is the count of the total days during the summer that year. Further arrangement of formula (2) gives:

$$\begin{aligned} Vis &= Vis_{normal} + (Vis_{WPSH} - Vis_{normal}) \times N_{WPSH}/N \\ &= Vis_{normal} \times [1 + B] \end{aligned} \quad (3)$$

where

$$B = (Vis_{WPSH} - Vis_{normal})/Vis_{normal} \times (N_{WPSH}/N) \times 100\%. \quad (4)$$

[40] Decomposition of the Vis into two terms as shown in formula (3) facilitates the study of the separate effects of emissions and RH on the trend of Vis. Because Vis_{normal} is Vis on days when RH is low, its trend largely reflects the effect of aerosol dry mass concentration and thus the effect of emissions (as the aerosol dry mass is strongly influenced by emissions). In contrast, by normalizing the difference of Vis_{WPSH} and Vis_{normal} with respect to Vis_{normal} [as shown in formula (4)] in the *same* summer (in which emissions on each day can be assumed as same), term B minimizes the complicating effect from yearly variation of emissions and thus expresses the RH effect on Vis due to the change in the occurrence of WPSH-controlled days in each summer. Hence, term B reflects the contribution of the change of WPSH (or RH) to the decline of Vis, and hereafter B is referred to as WPSH-type meteorological factor. Consequently, by computing Vis_{normal} and B in each summer and then calculating their trends, we can understand how the trend of emissions and RH separately influence the total trend of Vis in summer. With similar reasoning, we also compute the Vis_{normal} and B for winter; in this calculation, the criteria for WPSH-type meteorological days are similar to that in summer except that the temperature needs to be adjusted to accommodate the lower temperatures of winter. It should be noted that in winter, the stable and humid weather conditions are not related to WPSH, but to compare with summer, here we keep the term "WPSH-type meteorology."

[41] Further comparison between summer and winter indicates that over eastern China, the number (frequency) of humid and stable (low wind speed) Vis impairment days, or Vis impairment days associated with WPSH-type meteorology in winter generally is much smaller than that in summer (Figure 9a); the temporal trend of the number of Vis impairment days associated with WPSH-type meteorology in winter (+0.34 days per decade) is also much smaller than that in summer (+2.3 days per decade), all at a statistically significant level ($P < 0.001$). Consequently, the contribution of WPSH-type meteorological days to the trend of Vis (i.e., term B) in summer increases from about −2.6% in the 1970s to about −4.4% in the 2000s, with a linear decline trend of −0.48% per decade (Figure 9c), all of which are more negative than their respective counterparts (−1.7%, −2.7%, and −0.27% per decade) in winter (Figure 9d). Comparison of Figures 9a, 9c, and 9d implies that more frequent and rapid increase of summertime WPSH-type meteorology could be at least a partial cause of the more evident

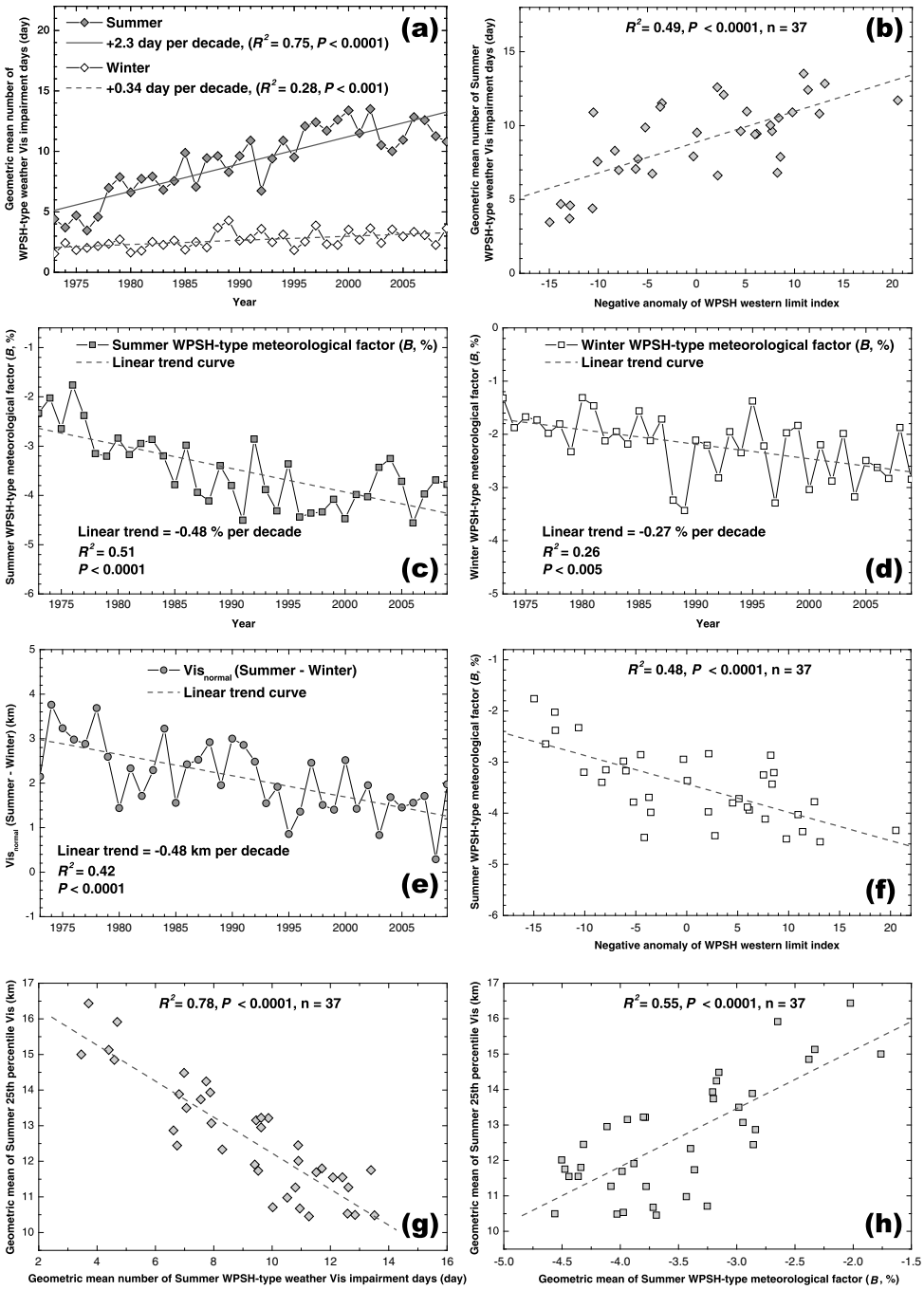

Figure 9. (a) 1973 – 2009 time series of mean number (over all the stations in eastern China) of WPSH-type weather Vis impairment days in summer and winter. (c) Same as Figure 9a but for the summertime WPSH-type meteorological factor, B, as defined in formula (4) in section 4.5 of the text. (d) Same as Figure 9a but for the wintertime WPSH-type meteorological factor, (B). (e) Same as Figure 9a but for the difference of Vis on normal (without WPSH-type weather) days between summer and winter, [Vis_{normal} (Summer − Winter)]. (b) Scatterplot of the geometric mean number of WPSH-type weather Vis impairment days (y-axis) against the negative anomaly of the western limit index (NAWI) of WPSH in summer. (f) Same as Figure 9b but for the WPSH-type meteorological factor (B). (g) Same as Figure 9b but for the geometric mean of the 25th percentile Vis (y-axis) against the geometric mean number of WPSH-type weather Vis impairment days. (h) Same as Figure 9b but for the geometric mean of the 25th percentile Vis (y-axis) against the geometric mean of the WPSH-type meteorological factor (B); all the scatterplots are based on results over eastern China in summer during 1973 – 1999. In all panels, the best linear fitting line (dash line) between the variations of the variables on the y-axis and x-axis is also shown, together with the relevant statistics including the square of linear correlation coefficient (R^2) and statistical significance (P). For the definition of geometric mean, refer to section 4.1 and Figure 4.

Table 2. Comparison of the Visibility (Vis, Unit: km) Decline Due to the WPSH Events in the 1970s and in the Most Recent Years

Date of the WPSH Weather Day	WPSH Events in the 1970s			Date of the WPSH Weather Day	WPSH Events in the Most Recent Years		
	Vis_{WPSH}[a]	Vis_{normal}[b]	ΔVis[c]		Vis_{WPSH}	Vis_{normal}	Δvis
11 July 1979	13.9	18.5	−4.6	24 August 2009	12.2	16.5	−4.3
24 June 1979	13.9	19.7	−5.8	22 June 2007	8.1	11.8	−3.7
04 August 1978	15.4	19.4	−4.0	18 August 2007	9.2	13.5	−4.3

[a]Vis on the WPSH weather day.
[b]Average Vis during the five days before the WPSH weather day.
[c]Vis decline due to WPSH weather ($\Delta Vis = Vis_{WPSH} - Vis_{normal}$).

Vis decline trend in summer than in winter. However, two questions still remain: (1) do emission trends contribute to the more dramatic Vis decline trend of summer, and (2) is our analysis of WPSH-type meteorological days consistent with the intensification and westward extension of WPSH as revealed in past studies?

[42] To evaluate the contribution of emissions to Vis trends, we analyze the trend of Vis_{normal} difference between summer and winter (Figure 9e). Although Vis_{normal} in both summer and winter shows a decreasing trend, the summertime Vis_{normal} decline is more rapid than that in winter (figures not shown). Consequently, the Vis_{normal} difference between summer and winter [Vis_{normal} (Summer − Winter)] shows a declining trend of −0.48 km per decade (Figure 9e). One reason for this result is that a majority of the daily summertime PM concentration varies in the "VPSA," within which increase of the PM concentration can result in a more obvious Vis decline as discussed in section 4.2. There may be other reason that the increase in the rate of summertime emissions is probably larger than that in the winter, (although the proportion of anthropogenic emissions of the major pollutants in summer is generally less than that in winter [see *Streets et al*., 2003, Figure 7 and *Zhang et al*., 2009, Table 9]). However, the latter needs further study. In fact, the increasingly strict regulation of winter home heating emissions that have been adopted in recent years as well as the increased use of air conditioning in recent summers in China should be considered (it is reported that electricity consumption in Chinese cities can increase dramatically with the rise of temperature on hot summer days in recent years; when the temperature was over 30°C, the electric power load in Beijing increased 5.7% for every 1°C increase in temperature in summer 2010, http://news.sina.com.cn/c/2010-07-19/044517826268s.shtml). The analyses above imply that the changes in PM concentration and emissions might be another cause of the more evident Vis decline trend in summer.

[43] Comparison of Vis decline due to the similar WPSH events in summer between those in the first decade of the study period (i.e., the 1970s) and those in the most recent years (Table 2, also see the supporting information Figure S1 for the meteorology) can also supply useful information about the contribution of increased emissions (and subsequently increased PM concentration) to Vis decline. For the selected WPSH events in the 1970s, Vis declined from an average value of 18.5 – 19.7 km during the five days before the WPSH weather day to 13.9 – 15.4 km on the WPSH weather day. While for the WPSH events selected in the most recent years, Vis declined from an average value of 11.8 – 16.5 km during the five days before the WPSH weather day to 8.1 – 12.2 km on the WPSH weather day. This comparison suggest that (1) the WPSH related stable weathers has led to Vis decrease both in the 1970s and in the most recent years; (2) the presumably higher PM concentration in the most recent years has resulted in a relatively lower Vis both on the WPSH weather day and on the normal days (compared to the Vis level in the 1970s). That is, the total Vis level in the recent years is generally lower than that in the 1970s. In this context, the stable weathers associated with WPSH can lead to further decrease of the already low Vis in the recent years. Note here the WPSH weather days (used in this comparison) are selected by subjectively inspecting and evaluating the daily meteorology in the first and last decades of the study period.

[44] To further link our analysis of WPSH-type meteorological days with the variation of WPSH, we calculate the correlation of the number of WPSH-type weather Vis impairment days and term *B* with the WPSH index. The number of WPSH-type weather Vis impairment days is significantly positively correlated with the NAWI of WPSH ($R^2 = 0.49$, $P < 0.0001$ significance, n = 37, Figure 9b), and term *B* in each year is significantly negatively correlated with NAWI ($R^2 = 0.48$, $P < 0.0001$ significance, n = 37, Figure 9f) over eastern China in summer during 1973 – 2009.

[45] Moreover, the number (frequency) of WPSH-type weather Vis impairment days and WPSH-type meteorological factor (*B*), both of which also reflect the variation of WPSH, shows strong ($R^2 = 0.78$, $P < 0.0001$ significance, n = 37, Figure 9g) and moderate ($R^2 = 0.55$, $P < 0.0001$ significance, n = 37, Figure 9h) correlation with the summertime Vis over eastern China during 1973 – 1999, respectively. Hence, the results presented in Figure 9 quantitatively show that the intensification and westward expansion of WPSH results in more episodes of Vis impairment and amplifies the effect of emission increases on summertime Vis decrease over eastern China.

5. Conclusions and Discussions

[46] Vis decrease in China has been mostly attributed to the increase of aerosol emissions [*Che et al*., 2007; *Chang et al*., 2009; *Wang et al*., 2009]. However, numerical model simulations have also suggested the importance of considering the change of weather systems accompanying climate change to study the change of air quality [*Jacob and Winner*, 2009]. This study gives an observational support of climate impact on Vis in eastern China. It shows that the decrease of Vis in China in the past three decades has a strong seasonal and geographical variation, with the largest decrease concentrated in eastern China in summer.

[47] Comparison with winter suggests three possible reasons for the more substantial Vis decline that has been observed over eastern China in summer: (1) a significant RH effect on Vis decrease has occurred due to the more frequent and rapid increase in summertime WPSH-type meteorology in recent years; (2) a majority of the daily summertime PM concentration varies in the "VPSA," within which an increase of the PM concentration can result in a more obvious Vis decline (section 4.2), with the increased occurrence of the summertime WPSH-type meteorology providing favorable stable weather conditions for the accumulation of pollution and increased PM concentration; and (3) the likely greater increase in the rate of emissions in summer compared to winter (discussed in section 4.5).

[48] Our study indicates that in addition to the increase in emissions, the strengthened and westward-extended WPSH since the late 1970s (associated with thermodynamically stable, hot and humid weather) also contributes to the larger Vis decrease in summer over eastern China; it leads to more episodes of Vis impairment and amplifies the Vis decline due to the increase of emissions alone. Taking the role of WPSH into account is helpful in understanding the recent episodes of summertime Vis degradation in various major cities in eastern China [*Wang et al*., 2002; *Fan et al*., 2005] as well as predicting future changes of visibility.

[49] Given that WPSH has strengthened and extended westward since the late 1970s [*Hu* 1997; *Chang et al*., 2000; *Gong and Ho*, 2002; *He and Gong*, 2002; *Zhou et al*., 2009] and might continue to intensify (or move poleward) in a warming climate [*Vecchi et al*., 2006; *Lu et al*., 2008], it is expected that the Vis decrease over eastern China in summer will likely continue even if aerosol emissions remain unchanged.

[50] For future work, more detailed analysis (especially through modeling) is still warranted to better understand how the processes associated with WPSH (such as more stable boundary layer, increase of RH and temperature, less clouds/stronger solar radiation, and therefore more efficient photochemical reactions) contribute to the Vis decrease, and to separate such contribution from the effect of emission increases. Moreover, the role of other possible factors in visibility decline also needs to be further studied.

[51] This study only focuses on how the variation of WPSH influences the summertime Vis trend over eastern China in the last three decades. The implication of this study, however, is global, because significant changes in climate appear to have been occurring and will continue to occur at various regions around the globe [*IPCC*, 2007]. It is thus crucial to consider changes in synoptic-scale weather systems as well as changes in anthropogenic emissions when assessing possible impacts on air quality and visibility posed by climate change.

[52] **Acknowledgments.** Wenjun Qu is grateful to Prof. Xiaoye Zhang from Chinese Academy of Meteorological Sciences for his continuous encouragement and support. Thanks to Amy L. Kessner for language editing and group members from University of Nebraska-Lincoln for their help during the work. The visibility data are from the National Climatic Data Center. This research is supported by the National Basic Research Program of China (2011CB403401), NSFC 41276009, Chinese Meteorological Administration's project GYHY(QX)201106006, and Chinese Ministry of Education's 111 Project (B07036).

References

Chang, C. P., Y. S. Zhang, and T. Li (2000), Interannual and interdecadal variations of the East Asian summer monsoon and tropical Pacific SSTs. Part II: Meridional structure of the monsoon, *J. Clim.*, *13*, 4326–4340.

Chang, D., Y. Song, and B. Liu (2009), Visibility trends in six megacities in China 1973–2007, *Atmos. Res.*, *94*, 161–167.

Che, H., X. Zhang, Y. Li, Z. Zhou, and J. J. Qu (2007), Horizontal visibility trends in China 1981–2005, *Geophys. Res. Lett.*, *34*, L24706, doi:10.1029/2007GL031450.

Cheung, H. C., T. Wang, K. Baumann, and H. Guo (2005), Influence of regional pollution outflow on the concentrations of fine particulate matter and visibility in the coastal area of southern China, China, *Atmos. Environ.*, *39*, 6463–6474.

China Meteorological Administration (2003), *Specifications for surface meteorological observation* [in Chinese], 151 pp., China Meteorol. Press, Beijing.

China Meteorological Administration (2010), *Visibility grade and forecast* [in Chinese], 7 pp., China Meteorol. Press, Beijing. Press.

Corfidi, S. F. (1996), The development and movement of warm-season haze over the central and eastern United States, *Natl. Weather Dig.*, *20*(3), 2–14.

Deng, X. J., X. X. Tie, D. Wu, X. J. Zhou, X. Y. Bi, H. B. Tan, F. Li, and C. L. Jiang (2008), Long-term trend of visibility and its characterizations in the Pearl River Delta (PRD) region, China, *Atmos. Environ.*, *42*, 1424–1435.

Fan, Y. Q., E. J. Li, and Z. L. Fan (2005), Visibility trends in 11 cities of Hebei province during 1960–2002 [in Chinese with English abstract], *Chin. J. Atmos. Sci.*, *29*(4), 526–535.

Gao, S. T., Y. S. Zhou, T. Lei, and J. H. Sun (2005), Analyses of hot and humid weather in Beijing city in summer and its dynamical identification, *Sci. in China, Ser. D*, *48*(S2), 128–137.

Gong, D. Y., and C. H. Ho (2002), Shift in the summer rainfall over the Yangtze River Valley in the late 1970s, *Geophys. Res. Lett.*, *29*(10), 1436, doi:10.1029/2001GL014523.

Gong, D. Y., S. W. Wang, Y. W. Yang, and Z. G. Zhao (1998), Analysis on the anomalous western Pacific subtropical high during the 1990s [in Chinese with English abstract], *Meteorol. Monogr.*, *24*(8), 8–13.

He, X. Z., and D. Y. Gong (2002), Interdecadal change in western Pacific subtropical high and climatic effects, *J. Geogr. Sci.*, *12*, 202–209.

Hu, Z. Z. (1997), Interdecadal variability of summer climate over East Asia and its association with 500 hPa height and global sea surface temperature, *J. Geophys. Res.*, *102*(D16), 19,403–19,412, doi:10.1029/97JD01052.

Husar, R. B., J. M. Holloway, D. E. Patterson, and W. E. Wilson (1981), Spatial and temporal pattern of eastern U.S. haziness: A summary, *Atmos. Environ.*, *15*(11), 1919–1928.

Intergovernmental Panel on Climate Change (IPCC) (2007), *Climate Change 2007: The Physical Science Basis. Contribution of Working Group I to the Fourth Assessment Report of the Intergovernmental Panel on Climate Change*, edited by S. Solomon et al., 996 pp., Cambridge Univ. Press, New York.

Jacob, D. J., and D. A. Winner (2009), Effect of climate change on air quality, *Atmos. Environ.*, *43*, 51–63.

Kalnay, E., et al. (1996), The NCEP/NCAR 40-year reanalysis project, *Bull. Am. Meteorol. Soc.*, *77*(3), 437–471.

Li, X. (2010), Effect of changing of ground weather monitoring specification in 1980 on visibility data continuity [in Chinese with English abstract], *Meteorol. Monogr.*, *36*(3), 117–122.

Lu, J., G. Chen, and D. M. W. Frierson (2008), Response of the zonal mean atmospheric circulation to El Niño versus global warming, *J. Clim.*, *21*, 5835–5851.

Mu Q. Z., S. W. Wang, J. H. Zhu, and D. Y. Gong (2001), Variations of the western Pacific subtropical high in summer during the last 100 years [in Chinese with English abstract], *Chin. J. Atmos. Sci.*, *25*(6), 787–797.

Qian, Y., D. Gong, J. Fan, L. R. Leung, R. Bennartz, D. Chen, and W. Wang (2009), Heavy pollution suppresses light rain in China: Observations and modeling, *J. Geophys. Res.*, *114*, D00K02, doi:10.1029/2008JD011575.

Qiu, J. H., and L. Q. Yang (2000), Variation characteristics of atmospheric aerosol optical depths and visibility in North China during 1980–1994, *Atmos. Environ.*, *34*, 603–609.

Qu, W. J., R. Arimoto, X. Y. Zhang, C. H. Zhao, Y. Q. Wang, L. F. Sheng, and G. Fu (2010), Spatial distribution and interannual variation of surface PM_{10} concentrations over eighty-six Chinese cities, *Atmos. Chem. Phys.*, *10*, 5641–5662.

Schichtel, B. A., R. B. Husar, S. R. Falke, and W. E. Wilson (2001), Haze trends over the United States, 1980–1995, *Atmos. Environ.*, *35*, 5205–5210.

Si, F. Q., J. G. Liu, P. H. Xie, Y. J. Zhang, W. Q. Liu, H. Kuze, C. Liu, N. Lagrosas, and N. Takeuchi (2005), Determination of aerosol extinction coefficient and mass extinction efficiency by DOAS with a flashlight source, *Chin. Phys.*, *14*, 2360–2364.

Streets, D. G., et al. (2003), An inventory of gaseous and primary aerosol emissions in Asia in the year 2000, *J. Geophys. Res.*, *108*(D21), 8809, doi:10.1029/2002JD003093.

Tai, A. P. K., L. J. Mickley, and D. J. Jacob (2010), Correlations between fine particulate matter ($PM_{2.5}$) and meteorological variables in the United States: Implications for the sensitivity of $PM_{2.5}$ to climate change, *Atmos. Environ.*, *44*, 3976–3984.

Tao, S. Y., and S. Y. Xu (1962), Circulation characteristics in association with persistent summer drought and flood in the Yangtze-Huaihe River reaches, *Acta Meteorol. Sin.*, *32*, 1–18.

Vecchi, G. A., B. J. Soden, A. T. Wittenberg, I. M. Held, A. Leetmaa, and M. J. Harrison (2006), Weakening of tropical Pacific atmospheric circulation due to anthropogenic forcing, *Nature*, *441*, 73–76, doi:10.1038/nature04744.

Wang, J. Z., X. D. Xu, and Y. Q. Yang (2002), A study of characteristics of urban visibility and fog in Beijing and the surrounding area [in Chinese with English abstract], *J. Appl. Meteorol. Sci.*, *13*, suppl., 160–169.

Wang, J., D. J. Jacob, and S. T. Martin (2008), Sensitivity of sulfate direct climate forcing to the hysteresis of particle phase transitions, *J. Geophys. Res.*, *113*, D11207, doi:10.1029/2007JD009368.

Wang, K. C., R. E. Dickinson, and S. L. Liang (2009), Clear sky visibility has decreased over land globally from 1973 to 2007, *Science*, *323*, 1468–1470.

Xu, M., C.-P. Chang, C. Fu, Y. Qi, A. Robock, D. Robinson, and H. Zhang (2006), Steady decline of east Asian monsoon winds, 1969–2000: Evidence from direct ground measurements of wind speed, *J. Geophys. Res.*, *111*, D24111, doi:10.1029/2006JD007337.

Xu, J., X. Yi, and J. Wang (2008), Analysis of climatic characteristics of high temperature and muggy weather in Liaocheng City [in Chinese with English abstract], *J. Anhui Agric. Sci.*, *36*(30), 13,293–13,294.

Zhang, S. Y., S. R. Wang, Y. S. Zhang, D. K. Zhang, and Y. L. Song (2004), The climatic character of high temperature and the prediction in the large cities of east of China [in Chinese with English abstract], *J. Trop. Meteorol.*, *20*, 750–760.

Zhang, X. Y., Y. Q. Wang, X. C. Zhang, W. Guo, and S. L. Gong (2008), Carbonaceous aerosol composition over various regions of China during 2006, *J. Geophys. Res.*, *113*, D14111, doi:10.1029/2007JD009525.

Zhang, Q., et al. (2009), Asian emissions in 2006 for the NASA INTEX-B mission, *Atmos. Chem. Phys.*, *9*, 5131–5153.

Zhang, Q. H., J. P. Zhang, and H. W. Xue (2010), The challenge of improving visibility in Beijing, *Atmos. Chem. Phys.*, *10*, 7821–7827.

Zhang, X. Y., Y. Q. Wang, T. Niu, X. C. Zhang, S. L. Gong, Y. M. Zhang, and J. Y. Sun (2012), Atmospheric aerosol compositions in China: spatial/temporal variability, chemical signature, regional haze distribution and comparisons with global aerosols, *Atmos. Chem. Phys.*, *12*, 779–799.

Zhou, T. J., et al. (2009), Why the western Pacific subtropical high has extended westward since the late 1970s, *J. Clim.*, *22*, 2199–2215.

Zhu, B. Q., and S. L. Mei (2010), A comparison of the automated visibility monitoring with man-made observation [in Chinese], *J. Zhejiang Meteorol.*, *31*(2), 25–28.

Auxiliary Material for
Effect of the strengthened western Pacific subtropical high on summer visibility decrease over eastern China since 1973.

Wenjun Qu,[1,2] Jun Wang,[2] Shanhong Gao,[1] and Tongwen Wu[3]

[1]Physical Oceanography Laboratory, Key Laboratory of Ocean-Atmosphere Interaction and Climate in Universities of Shandong, Ocean University of China, Qingdao 266100, China

[2]Department of Earth and Atmospheric Sciences, University of Nebraska-Lincoln, Lincoln, Nebraska 68588-0340, USA

[3]National Climate Center, China Meteorological Administration, Beijing 100081, China

Journal of Geophysical Research, Atmospheres, 2013

Introduction

This supplementary figure (Figure S1) presents comparison of the spatial coverage of WPSH and related visibility (Vis) decline between WPSH events in the first decade of the study period (the 1970s) and WPSH events in the most recent years. The Vis decline due to the WPSH weather (ΔVis) shown upper left of each panel is calculated by the difference of Vis on the specific WPSH weather day and the average Visd uring the five days before the WPSH weather. Comparison is made between (top) July 11, 1979 and August 24, 2009, (middle) June 24, 1979 and June 22, 2007, and (bottom) August 4, 1978 and August 18, 2007. The red contour lines in each panel show daily geopotential height (gpm) at 500 hPa on the specific day with WPSH weather. The meteorological data used is from NCEP global reanalysis (http://www.esrl.noaa.gov/psd/data/gridded/data.ncep.reanalysis.pressure.html).

1. fs01.pdf Comparison of the spatial coverage of WPSH and related visibility (Vis) decline between WPSH events in the first decade of the study period (the 1970s) and WPSH events in the most recent years.

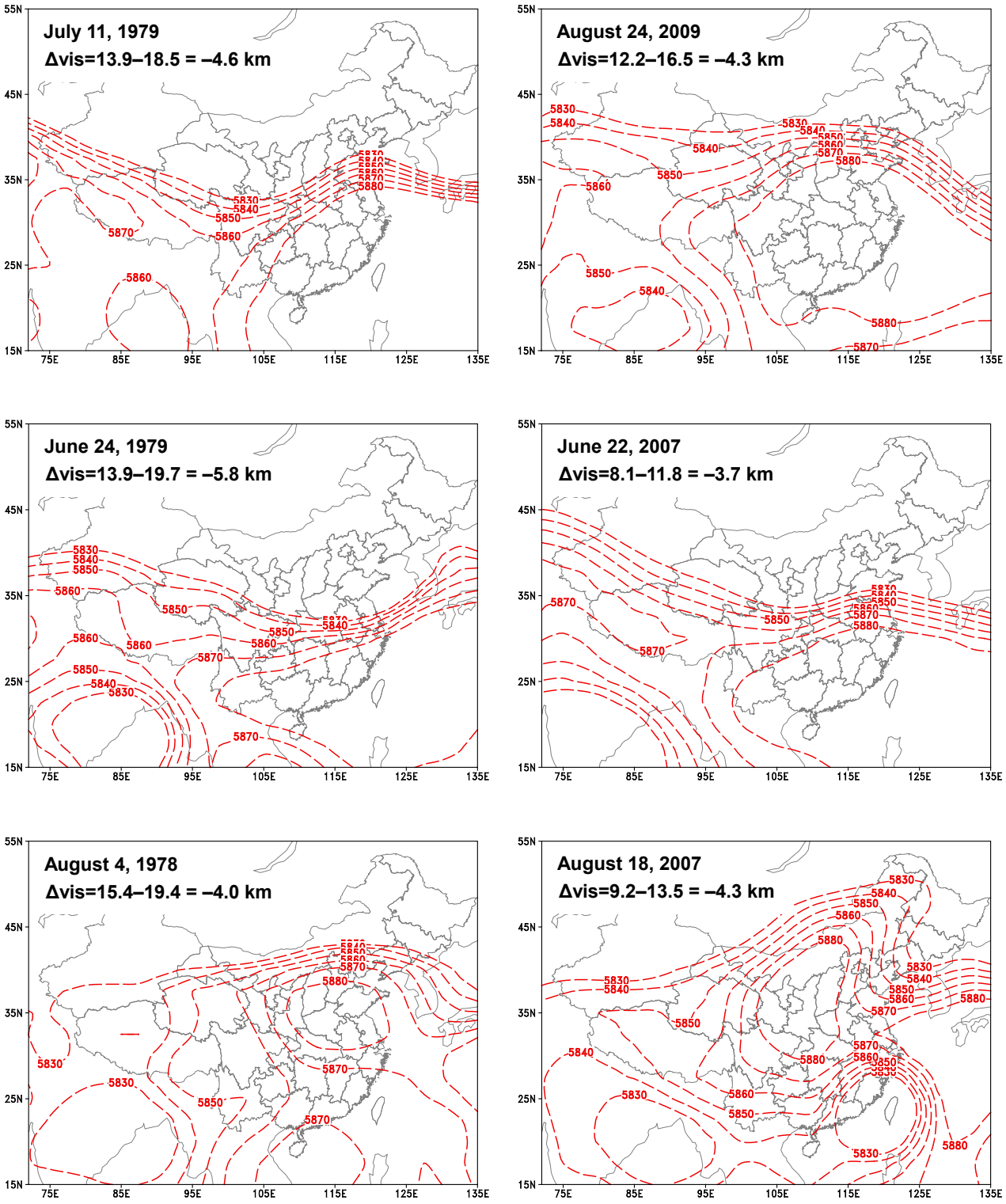

Figure S1. Comparison of the spatial coverage of WPSH and related visibility (Vis) decline between WPSH events in the first decade of the study period (the 1970s) and WPSH events in the most recent years. The Vis decline due to the WPSH weather (ΔVis) shown upper left of each panel is calculated by the difference of Vis on the specific WPSH weather day and the average Vis during the five days before the WPSH weather. Comparison is made between (top) July 11, 1979 and August 24, 2009, (middle) June 24, 1979 and June 22, 2007, and (bottom) August 4, 1978 and August 18, 2007. The red contour lines in each panel show daily geopotential height (gpm) at 500 hPa on the specific day with WPSH weather. The meteorological data used is from NCEP global reanalysis (http://www.esrl.noaa.gov/psd/data/gridded/data.ncep.reanalysis.pressure.html).